Pergamon

Int. J. Heat Mass Transfer. Vol. 38, No. 4, pp. 607–613, 1995

0017-9310/95 $9.50+0.00

0017-9310(94)00281-9

Finite-element method analysis of interaction effects for vaporising cylinders arranged in triangular configurations

S. K. BANERJI, K. SIVASANKARAN, K. N. SEETHARAMU and R. NATARAJAN†

Department of Mechanical Engineering, Indian Institute of Technology, Madras, 600 036, India

(*Received* 5 *August* 1991 *and in final form* 18 *August* 1994)

Abstract—The interaction effect between vaporising cylinders arranged in three different triangular configurations, under quasi-steady non-convective conditions, has been determined by employing the finite-element method. The interaction effects are expressed in terms of the variation of the interaction coefficient with inter-particle separation, and the iso-density contours. It is seen that, while the interaction coefficients for all the cylinders increase with spacing, they are lower for cylinders which are surrounded by other cylinders.

INTRODUCTION

Interference effects among the burning drops comprising a burning or vaporizing liquid fuel spray need to be assessed before a thorough description of spray combustion can be achieved. Several studies have been undertaken recently to quantify the deviations from isolated single drop vaporization or combustion behavior [1–7]. In all of the above studies, the problem is reduced to the solution of the Laplace equation in the appropriate geometry. While Brzustowski *et al.* [3] and Umemura *et al.* [6,7] have utilized the bispherical coordinate system to solve the problem, Labowsky [1, 2, 4, 5] has employed the modified images method for obtaining the solution. While the former method is restricted to a system of two droplets, the latter method may be extended to arrays of more droplets.

In the present work, the interference effects between neighboring cylinders undergoing vaporization have been analyzed utilizing Labowsky's approach for problem formulation, leading to the Laplace equation, and employing the finite-element method (FEM) for solving it.

PRESENT WORK

Formulation

The set of assumptions normally applied for investigating non-convective quasi-steady vaporization is employed here. The arrays of cylinders considered are shown in Figs. 1–3. Figures 4–6 depict the computational domain, and Fig. 7 shows an enlarged view of the finite-element mesh for configuration 1, indicating the smooth transition from a coarse mesh to a fine mesh as the drop surface is approached.

The governing equation for the vapor density in an array, in the absence of Stefan flow, is the Laplace equation. Introducing the dimensionless vapor density ρ^*, the governing equation is

$$\nabla^2\rho^* = 0. \tag{1}$$

with the following boundary conditions:

$\rho^* = 1$ on all particle surfaces

$\rho^* = 0$ far from the array.

The interaction coefficient for cylinders is defined by

$$\eta = \frac{\text{evaporation rate from interacting cylinder}}{\text{evaporation rate from an isolated cylinder of same size.}} \tag{2}$$

Labowsky [2] has shown that the interaction coefficient is the same with or without significant Stefan flow.

The evaporation rate for each cylinder is obtained by integrating the mass flux represented by the vapor pressure gradient over the surface of the cylinder.

Solution procedure

FEM has been employed in order to solve equation (1) for the different arrays of cylinders. The outer boundary is kept at 20 times the radius of the cylinder, since it was found that beyond this the results are not affected. The interaction coefficients for the different cylinders have been calculated by computing the

† Author to whom correspondence should be addressed.

NOMENCLATURE

D	drop diameter
k	burning constant
L	non-dimensional separation
$\dot{m}$	burning rate
t	time.

Greek symbols

η	interaction coefficient, $\dot{m}_{int}/\dot{m}_{iso}$
ρ	vapor density
ρ^*	dimensionless vapor density.

Subscripts

int	interacting drop
iso	isolated drop
s	drop surface
∞	far from the drop.

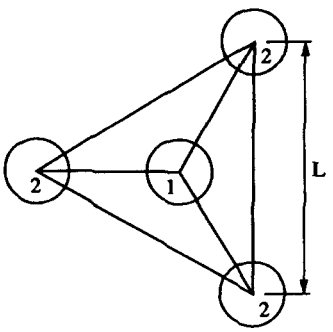

Fig. 1. Configuration 1 involving four cylinders.

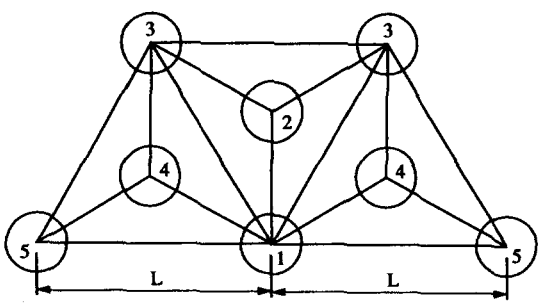

Fig. 2. Configuration 2 involving eight cylinders.

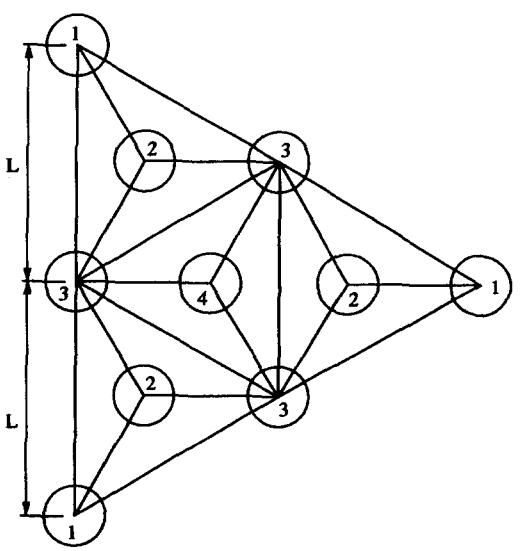

Fig. 3. Configuration 3 involving 10 cylinders.

derivatives of ρ^* in the radial direction and integrating over the surface of the cylinder under consideration. In view of the difficulties of mesh generation for a 3-D analysis, as a first step 2-D analysis is resorted to, thus restricting the applicability to infinitely long (equal-sized) cylinders, in three different configurations.

RESULTS AND DISCUSSION

Figure 8 shows the comparison of the present 2-D FEM analysis with Labowsky's 3-D analytical procedure for configuration 1. The interaction coefficient increases slowly with the non-dimensional distance, showing the reduction in interference effects with increasing separation. It is seen that, beyond $L \cong 7$, the difference is constant at about 11%, while the error is less at smaller separation. In view of the considerable reduction in computer time and effort, the 2-D analysis is attractive.

Figure 9 shows the comparison of Labowsky's 3-D results with the 2- and 3-D axisymmetric results obtained using the present procedures [8] for two cylinders/spheres. It is seen that, while there is good agreement (2%) between the two 3-D analysis, the 2-D analysis yields lower η values, the error decreasing with increasing L; the maximum error is about 12%.

Figure 10 shows the effect of L on η for the first configuration. While, for both cylinders 1 and 2, η increases with L, for cylinder 2 it varies from about 0.72 to 0.82 over $12D$, and for cylinder 1 it varies from about 0.19 to 0.60 over the same L. This is evidently because the latter is surrounded by three other vaporizing cylinders which suppress the vaporization from this cylinder.

In the formulation employed here, the interaction coefficient for vaporization is a function only of the non-dimensional separation distance. However, as pointed out by Xiong *et al.* [9], η is a function not only of instantaneous geometrical factors, but also of the initial and aerothermochemical aspects of the system.

Figure 11 shows the effect of non-dimensional separation L on η for the five different classes of cylinders in the second configuration. It can be seen that the location of the cylinder in the array, which determines the number of neighboring cylinders which interact

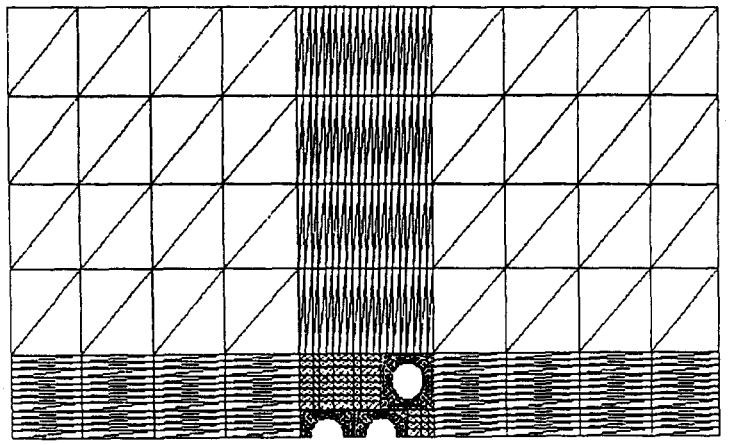

Fig. 4. Finite-element mesh for configuration 1.

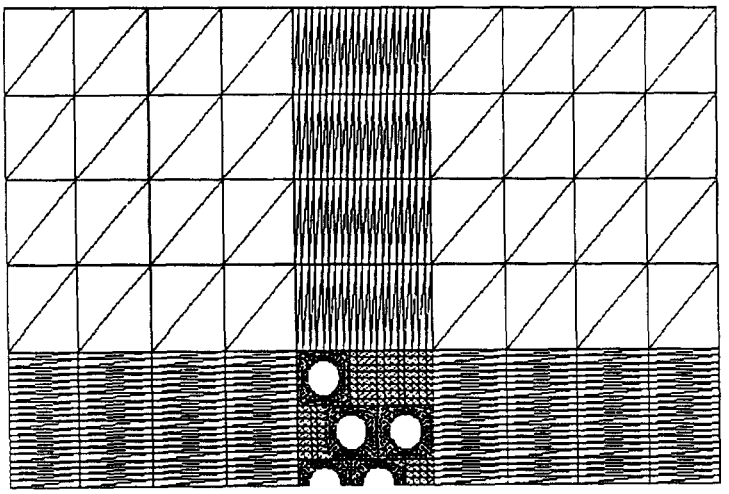

Fig. 5. Finite-element mesh for configuration 2.

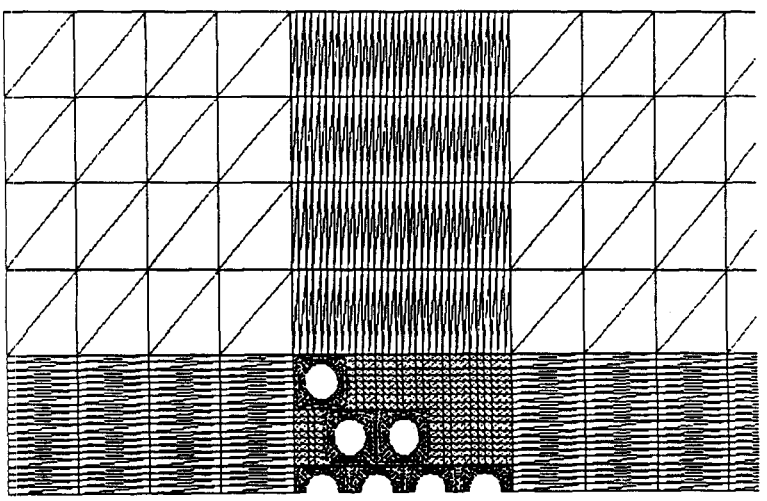

Fig. 6. Finite-element mesh for configuration 3.

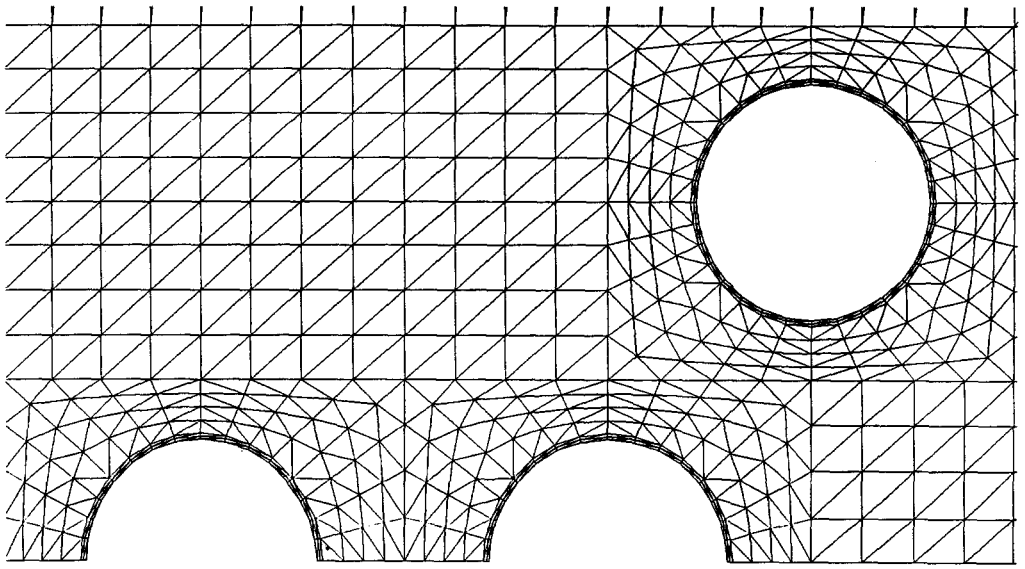

Fig. 7. Enlarged view of finite-element mesh for configuration 1.

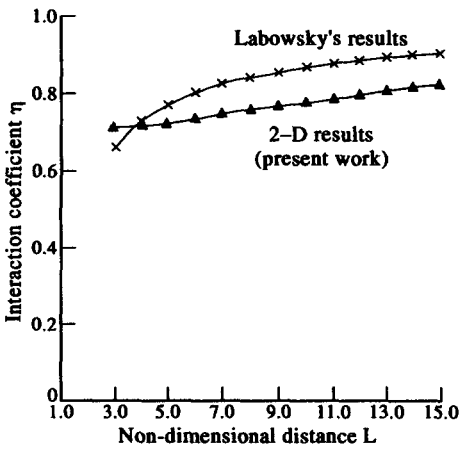

Fig. 8. Comparison of 2-D results with Labowsky's results.

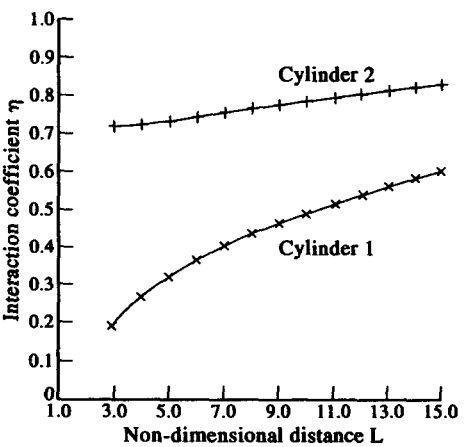

Fig. 10. Effect of non-dimensional distance on interaction coefficient for configuration 1.

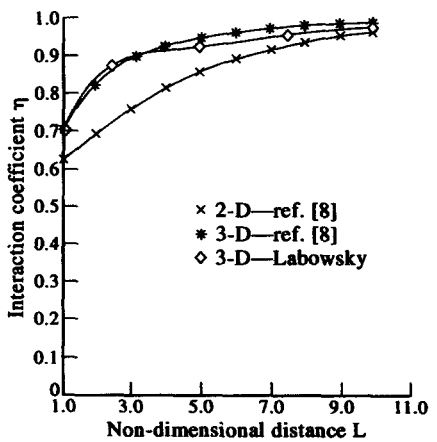

Fig. 9. Comparison of 2-D, 3-D and Labowsky's results for two droplets.

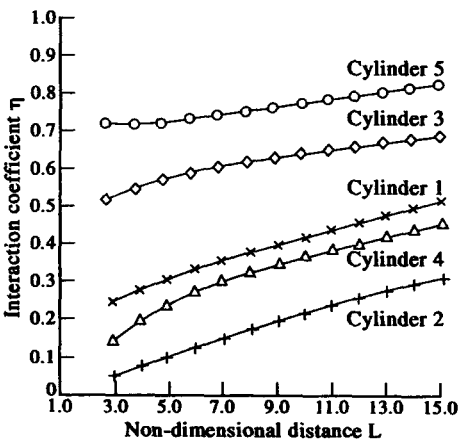

Fig. 11. Effect of non-dimensional distance on interaction coefficient for configuration 2.

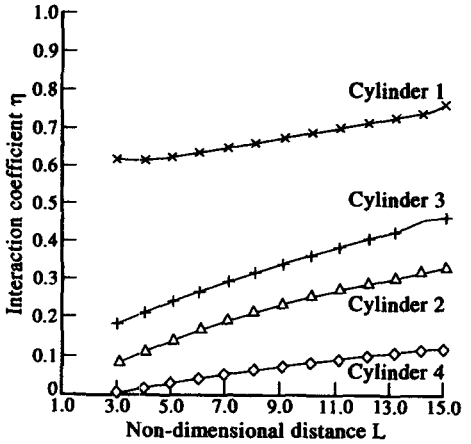

Fig. 12. Effect of non-dimensional distance on interaction coefficient for configuration 3.

with it, exerts a significant influence in determining the variation of η with L. The interaction coefficient for cylinder 5, which suffers the least interference, varies form 0.69 to 0.78, while for cylinder 2, which suffers the most interference, it varies from as low as 0.03 to about 0.27, over the same separation distance.

Figure 12 shows the variation of η with L for the six different classes of cylinders comprising the third configuration. While η for cylinders 1 or 7, which suffer the least interference, varies from 0.60 to 0.74, for cylinder 4, which suffers the most interference, η varies from as low a value as 0.003 to 0.123, over the same separation distance.

Figures 13 and 14 show the iso-density contours for configuration 1, for $L = 9$ and 15, respectively. The decreasing interaction between the vaporizing cylinders with increasing separation is evident from these contours.

Figure 15 shows the effect of spacing on the iso-density contours for configuration 2, again revealing that, with increasing separation, the interference effects decrease.

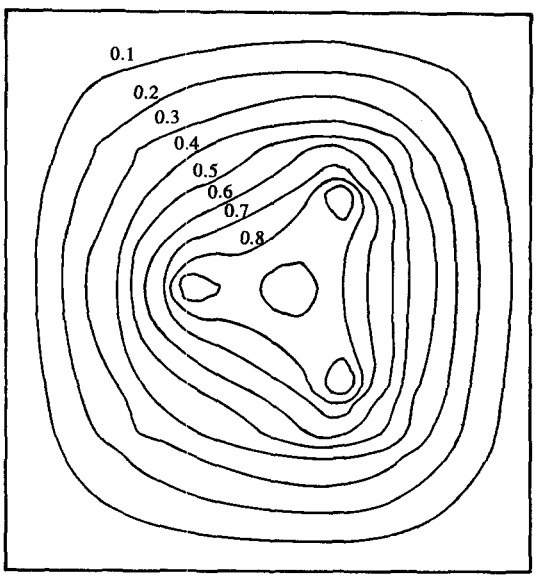

Fig. 13. Iso-density contours for configuration 1 ($L = 9$).

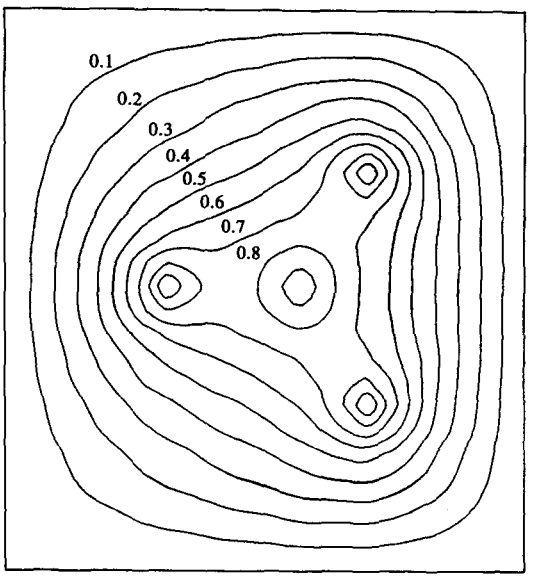

Fig. 14. Iso-density contours for configuration 1 ($L = 15$).

Figure 16 shows the iso-density contours for configuration 3 at $L = 20$. The corner cylinders suffer the least interference, while the central ones suffer more interference.

As far as the applicability of the D^2-law, which is valid for non-convective quasi-steady vaporization of isolated spheres (and cylinders), to interacting cylinders is concerned, since, by definition of η,

$$\frac{dD^2}{dt} = k_{iso}\eta \tag{3}$$

and since η varies with L, which increases as the cylinders vaporize, it is seen that the D^2-law is not valid for interacting cylinders.

CONCLUDING REMARKS

The three configurations chosen here represent a systematic building of arrays, which may be extended to large assemblages characteristic of spray drops. It is shown that the finite-element analysis offers a convenient generalized procedure for obtaining the overall evaporation rates, and hence interaction coefficients, even for complex configurations. The method has been first validated against the results obtained by Labowsky's analytical procedure for configuration 1.

It is seen that, with increasing inter-particle separation, the interaction coefficient increases slowly, indicating a reduction in the interference effect at large separation. In a multi-particle configuration, the inter-

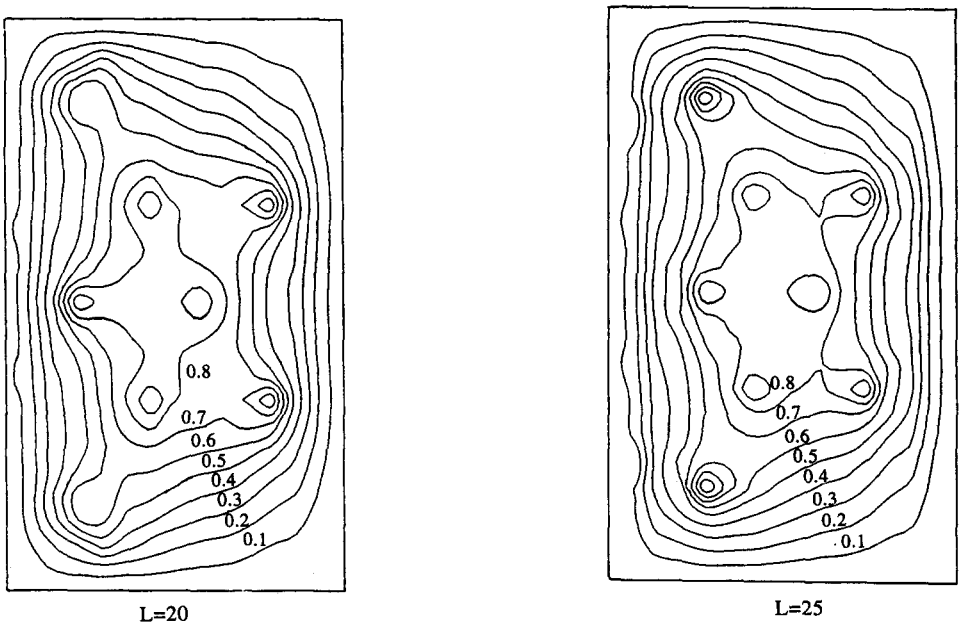

Fig. 15. Iso-density contours for configuration 2.

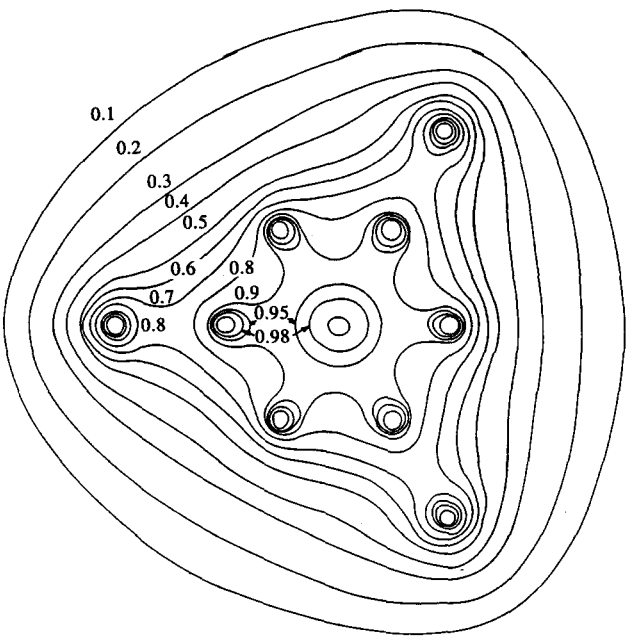

Fig. 16. Iso-density contours for configuration 3 ($L = 20$).

ference effect is maximum for the particle which is surrounded by the largest number of neighbors. It has also been possible to plot the iso-density contours, which provides an indication of the nature and extent of the interference effects.

It can be seen, however, that a considerable amount of work still needs to be done before these results can be applied to sprays; for example, extension to 3-D arrays, spheres, etc.

REFERENCES

1. M. Labowsky, The effects of nearest neighbor interactions on the evaporation rate of cloud of particles, *Chem. Engng Sci.* **31,** 803–813 (1976).
2. M. Labowsky, A formalism for calculating the evaporation rates of rapidly evaporating particles, *Combust. Sci. Technol.* **18,** 145–151 (1978).
3. T. A. Brzustowski, E. M. Twardus, S. Wojcicki and A. Sobiesiak, Interaction of two burning fuel droplets of arbitrary size, *AIAA J.* **17,** 1234–1242 (1979).

4. M. Labowsky, Transfer rate calculations for compositionally dissimilar interacting particles, *Chem. Engng Sci.* **35,** 1041–1048 (1980).
5. M. Labowsky, Calculation of the burning rates of interacting fuel droplets, *Combust. Sci. Technol.* **22,** 217–226 (1980).
6. A. Umemura, S. Ogawa and N. Oshima, Analysis of the interaction between two burning droplets, *Combust. Flame* **41,** 45–55 (1981).
7. A. Umemura, S. Ogawa and N. Oshima, Analysis of the interaction between two burning fuel droplets with different sizes, *Combust. Flame* **43,** 111–119 (1981).
8. K. Sivasankaran, FEM analysis of interaction effects for burning spheres and cylinders, M.Tech. Thesis, IIT, Madras (1990).
9. T. Y. Xiong, C. K. Law and K. Miyasaka, Interactive vaporization and combustion of binary droplet systems, *Twentieth Symposium (International) on Combustion*, pp. 1781–1787. The Combustion Institute (1984).